CHAPTER 12.2

Aluminum Extraction

Barry Welch and Halvor Kvande

More aluminum is produced today than all of the other nonferrous metals combined. The total world production of primary aluminum was close to 63 million t (metric tons) in 2017, and, in addition, around 20 million t were recycled. The country with the largest smelter production of aluminum is China, with about 56% of the global production, while the five largest aluminum producers in 2016 were Hongqiao (China), UC Rusal (Russia), Rio Tinto Alcan (Canada), Shandong Xinfa (China), and Chalco (China). There has been a significant growth in demand for aluminum in recent years, and the more conservative predictions are a growth at or above 5% per annum over the next decade. As a curiosity, of the 1 billion t of aluminum ever produced, it is estimated that about 75% is still in productive use.

Aluminum is second only to steel in annual production volume. With a density of 2.7 kg/dm^3 at room temperature, aluminum has only about one-third of the density of iron and steel and belongs to the so-called light metals. Besides the light weight, the properties that have enhanced the growth in its use include the ease of forming into simple or complex shapes by rolling, extrusion, or casting of a diverse range of alloys. Thus, the main cast house products are foundry alloys, extrusion ingots, sheet ingots, remelt ingots, and wire rod. The ability to form decorative and corrosion-protective surfaces gives a long low-maintenance life to the finished forms. Furthermore, aluminum has high electrical and thermal conductivity and excellent strength-to-weight ratio. These benefits are capped by the recyclability of almost all products formed from aluminum and its alloys. These properties have made it the world's most widely used nonferrous metal and have impacted and improved the quality of life for everyone. Usage examples range from the expansion in aircrafts and safe air travel that has been enabled by aluminum, the use of aluminum cables for bringing power to new productive and sustainable communities with lower energy losses, lightweight and easily manageable recreational marine and pleasure craft, and complex extruded shapes that have enabled architectural advances in energy-saving green building construction. Protective aluminum packaging enables preservation of precious nutritional and pharmaceutical resources, while the recyclability of aluminum beverage cans is well known. Although production of the metal is energy intensive, the net greenhouse gas emissions are lowered when used in the transport industry because of the reductions in weight and fuel consumption.

PRODUCTS SHIPPED FROM ALUMINUM SMELTERS

Pure aluminum is soft and ductile with limited strength, but by alloying with small amounts of other metallic elements, the properties of aluminum products can be modified to suit a wide diversity of applications. However, it is important for smelters to produce the aluminum to a high purity, so that the desired properties of the finished product after adding the selected alloy agents are not compromised. Typical impurities that can be co-deposited during the smelting process include the alkali metals present as components of the electrolyte, Fe and Si from either impurities in the smelter-grade alumina (SGA) or through corrosion of the cell components, and the metals of other oxide impurities that are precipitated with the alumina in the Bayer process. Although the alkali metals can be readily removed from the metal tapped from the cells—usually by a displacement reaction with aluminum fluoride—it is important to ensure that the SGA and work practices do not introduce the other reducible impurities. This is emphasized in Table 1, which summarizes the designation of the products shipped from the aluminum smelters, the purity requirements, and primary uses.

The two main groups of alloys are cast aluminum and wrought aluminum alloys. The main alloying elements used to impart specific properties on the finished product are copper, iron, manganese, magnesium, silicon, and zinc. These alloying elements impart different properties, making the product more suitable with respect to strength, weldability, casting, machinability, and corrosion resistance. For wrought aluminum alloys, the internationally accepted designation series are given in Table 2.

In Table 2, the first number in the series is simply to identify the key alloying element. The number 5 in the 5XXX

Barry Welch, Professor Emeritus, University of Auckland, Auckland, New Zealand
Halvor Kvande, Professor Emeritus, Norwegian University of Science & Technology, Trondheim, Norway

Table 1 Designation and purity specifications of aluminum shipped from smelters

As-Cast Products*	Purity	Primary Use	Shape/Size	Comments
P1020A	≥99.70%	Remelt for a wide range of products and alloys	Most common are T-shaped ingots of 20 kg to 750 kg in mass. Occasionally as square or round billet.	Commercial-grade purity; standard on the London Metals Exchange
P0610A	≥99.84%			Purity grade with little or no premium
P0507A	≥99.88%			High purity with premiums of tens of dollars per metric ton
P0506A	≥99.89%			
P0406A	≥99.90%			
P0404A	≥99.92%	Aerospace applications		Very high purity with premiums more than $100 per metric ton
P0303A	≥99.94%			
P0202A	≥99.96%			Super purity with premiums of hundreds of dollars per metric ton
99.97%–99.98%	≥99.97%–99.98%	Electronics, capacitor foil		Highest super-purity grade that can be produced in standard reduction cells
P1535A	≥99.5%	Common foil		Off-grade metal that is discounted by tens of dollars per metric ton
Letter grade	<99.5%	Common foil additive		Low-grade metal with discounts of more than $100 per metric ton for metal with >1% iron
Foundry alloy	Varies, typically >7% Si	Wheels for trucks and automobiles		Premium product that is high in silicon content
Conductor rod	Typically <0.03% Si	Conductor wire, transmission cable	Coiled rod	Premium product that is low in trace metals that detract from electrical conductivity

Data courtesy of the Aluminium Association

*P0202A through P1535A and others not shown in this table are commonly designated grades by the Aluminium Association. The first two numbers identify the maximum Si content. The last two numbers identify the maximum Fe content of the metal. Thus, P1020A has a maximum of 0.10% Si and 0.20% Fe. Other impurities including Zn, Ga, V, and "all others" may also have limits, especially on the higher-purity metal grades.

series simply means that the main alloying element is magnesium. In the 1XXX series of pure aluminum, the third and fourth numbers indicate the purity percentage of the aluminum above 99%. A1030 aluminum will then be 99.3% pure. In the higher-numbered series, the last two numbers are an identifier for a specific alloy.

As with other metal products, treatment changes the basic properties of the alloy. The alloys that can be heat treated are the 2XXX, 6XXX, and 7XXX series.

Table 2 Widely used alloy designation system for wrought aluminum alloys

Series	Major Alloying Elements	Changed Properties
1XXX	Al of minimum 99% purity	
2XXX	Al–Cu	Increased strength and improved machinability
3XXX	Al–Mn	Increased strength and hardness
4XXX	Al–Si	Improved ductility
5XXX	Al–Mg	Improved strength and corrosion resistance
6XXX	Al–Mg–Si	Improved stability to cast and corrosion resistance
7XXX	Al–Zn–(Mg)–(Cu)	Reduced ability to be cast and improved strength
8XXX	Al–Other elements	
9XXX	Unused series	

Data courtesy of the Aluminium Association

MODERN ALUMINUM ELECTROWINNING CELLS

The established process for electrowinning of aluminum revolves around the independent discoveries in 1886 and the subsequent patents of C.M. Hall (1886) and P.L.T. Héroult (1886). Fundamentally, the core features of the process have remained unchanged since, other than design, cell size, and refinements to operating conditions to enhance the energy efficiency and eliminate potentially harmful environmental impact.

The successful development of the aluminum industry has been achieved by merging two different industrial processes, namely, the extraction of a high-purity alumina from bauxite by the Bayer process, and the Hall–Héroult process for directly electrowinning a high-purity metal capable of satisfying the requirements for the range of applications. Resources of bauxites, the raw material for aluminum, are only located in seven areas: Western and Central Africa (mostly Guinea), South America (Brazil, Venezuela, and Suriname), the Caribbean (Jamaica), Oceania and Southern Asia (Australia and India), China, the Mediterranean (Greece and Turkey), and the Urals (Russia). The Bayer process is described in a separate chapter in this handbook but is integral to the success of the industry.

Aluminum does not occur in nature but rather in extremely stable combined forms, particularly oxides of which the weathered bauxite ore bodies present the easiest path for extraction in a pure form. Hence, the extraction of Al is reliant on the following general path:

$$Al_2O_3 + \text{reductant/energy} \Rightarrow 2Al + [O_2 \text{ or oxidized reductant}] \quad \textbf{(EQ 1)}$$

This process should be performed in a manner that prevents by-products interacting with the aluminum product, a constraint best satisfied using an electrochemical path since it provides a simple mechanism for separating the aluminum from the other products. Chemical conversion to intermediates such as aluminum chloride and aluminum oxycarbides to enable alternative paths for the final extraction step have been researched at length, but until now, both energetically and environmentally, the conditions are best satisfied by using

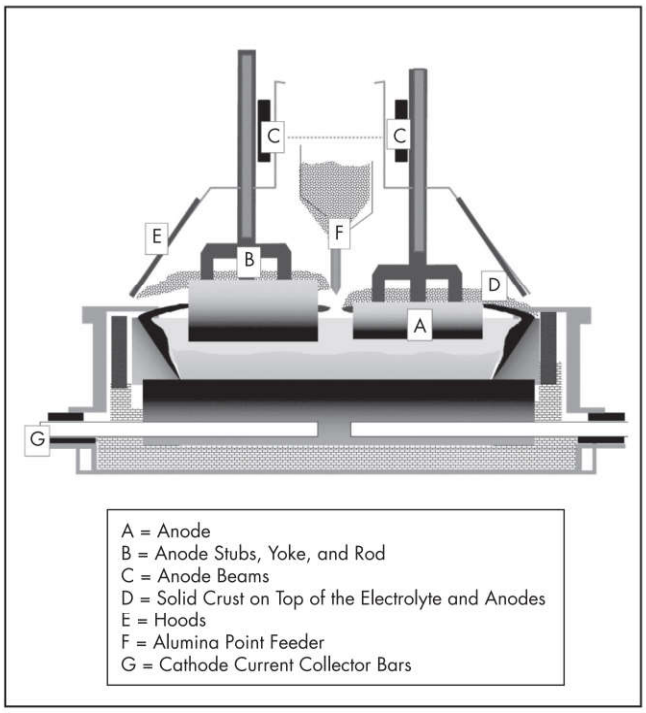

Figure 1 Common features of a modern aluminum electrolysis cell

carbon as a co-reductant. Operating the electrochemical cell at as low temperature as possible, but above the melting point of aluminum, is important because this enables the product to subsequently be delivered in an appropriate form.

Some of the very early electrowinning cells were externally heated and cylindrical in shape and, consequently, they were referred to as "pots," an expression that continues today. The process revolves around the electrochemical decomposition of alumina dissolved in a molten fluoride electrolyte that is dominated by sodium fluoride and aluminum fluoride proportioned to give stoichiometric compositions on the aluminum fluoride–rich side of cryolite, $3NaF{\cdot}AlF_3$. Consumable carbon anodes are used to lower the electrical energy requirements, and hence the operating electrochemical potentials. Because of the operating temperature that is necessary, it involves two liquid layers, the solvent electrolyte and the liquid aluminum cathode. Consequently, one of the challenges is to ensure that the density of the electrolyte is sufficiently lower than that of the metal to avoid inversions through magnetic or other forces that can be generated. A basic cross section showing the common features applicable to all modern aluminum cell designs is illustrated in Figure 1.

The objective is to produce the metal according to the following two reactions:

$$Al_2O_3\ (\text{dissolved}) + 3C(s) = 2Al(l) + 3CO(g) \quad \textbf{(EQ 2)}$$

$$Al_2O_3\ (\text{dissolved}) + 1.5C(s) = 2Al(l) + 1.5CO_2(g) \quad \textbf{(EQ 3)}$$

The process conditions are selected so that a maximum amount of metal is produced according to Equation 3, with the dominant electrochemical oxidation occurring on the horizontally oriented undersurface. The consumption of the anodes necessitates an engineering design to both steadily lower the anode assembly and also to periodically replace the spent anode "butt" (A in Figure 1) with a new rodded anode assembly. The assembly comprises a combination of a new carbon block, and the supporting aluminum rod stem plus a steel yoke assembly (B in Figure 1) that is cast into recesses in the top of the block for good electrical contact. Typically, only 70%–80% of the anode carbon introduced to the cell is consumed with the residual butt being reprocessed for recycling. Limiting the minimum size of the anode butt prevents electrolyte overflowing the upper surface and subsequently corroding the assembly contaminating the metal. The newly introduced cold anode gives a thermal disturbance and does not carry its normal share of current until the freeze formed during introduction has melted and the interface of the carbon assumes the correct anode–cathode distance. Consequently, the anodes are changed at regular time intervals and those within a cell are of varying ages so that there is a minimum disturbance to the cell at any one time. However, within a cell there will therefore be some spatial and temporal variations in properties.

As the metal pad height increases, the estimated production during the time interval is periodically siphoned out of the cell and simultaneously the anodes are lowered by the vertically movable anode support beam (C in Figure 1) to enable maintenance of the interelectrode distance at or near the target value. Typically, several metric tons of metal are siphoned from each cell at intervals between one and three days, the amount being dependent on the design height variation limits.

Prevention of air burn of the upper surfaces of the hot anodes has been a challenge, because there is the requirement to produce a high-purity metal, and potential contaminants must therefore be avoided. Today, the industry tends to use a powdered anode cover mixture (D in Figure 1) comprising a blend of alumina and electrolyte components. The spillage into the electrolyte does not introduce major disruptions or quality issues. The cover material blend also serves as a good thermal insulation enabling minimization of cell heat loss, and the interaction between vapors from the electrolyte and the electrolyte components in the cover material tends to sinter and minimize the potential for air access.

The SGA supplied by modern refineries contains approximately 5 mol % alumina monohydrate, boehmite, or, more correctly, the oxyhydroxide $Al_2O_2(OH)_2$. Much of the remaining alumina is of the gamma structure, which tends to absorb moisture. Consequently, there is some direct and indirect hydrolysis of the electrolyte-liberating hydrogen fluoride with the cell gases following alumina additions. It has been unequivocally established (Patterson 2002) that the hydroxyl ion is stable within the electrolyte, but during electrolysis, hydrogen fluoride is co-evolved at the anode according to the following equation:

$$1.5Al_2O_3{\cdot}H_2O + Na_3AlF_6(l) + 3C(s) = 4Al(l) + 3HF(g) + 3CO_2(g) + 3NaF(l) \quad \textbf{(EQ 4)}$$

To prevent the release of these gases to the atmosphere, modern cells are hooded (E in Figure 1) and the cells operate at a slightly reduced pressure to take the gases to an emissions scrubbing unit (a dry scrubber).

Maintenance of the dissolved concentration of alumina in the electrolyte is achieved by adding small amounts regularly according to a predictive control strategy aimed at achieving complete dissolution of the oxide in the electrolyte before it can sink beneath the metal pad. Consequently, all modern cells are fitted with point feeders (F in Figure 1), which add

a fixed volume of powder alumina equivalent to a specified weight between 1 and 2 kg per shot. The point feeders are located at regular intervals along the center channel of the cell with the number of feeders installed being influenced by the cell amperage.

The computer-generated model of a modern high-amperage cell technology given in Figure 2 demonstrates that the modern cell is vastly different to the early pots, with the lower section more closely resembling a "matchbox" with an overlying superstructure supporting the anodes, the alumina reservoir containers (bins), and the fume capture covers. That the cells have high length-to-width ratio is because the width is constrained by being limited to two rows of anodes.

Also shown in Figure 2 is the cell-to-cell interconnection busbars. Current is introduced to the cell by the four anode risers, and after passing through the electrolyte, it exits the cell via the cathode current collector bars (G in Figure 1), which are connected to the flat aluminum bars that surround the lower part of the cell. This cathode busbar provides interconnection to the anode risers of the next cell, as seen in the extreme right-hand side.

The voltage drop through the external busbar represents wasted energy, and consequently—subject to design and cost constraints—the cross-sectional areas are maximized and lengths minimized.

Each cell is self-heating and operated within the energy input that will maintain the electrolyte and electrode interfaces within a narrow band of the target temperature. However, it must also provide the thermal energy to preheat all materials introduced to the cell and the conversion energies for the various reactions that occur—not only for Equations 1 to 3 but also for secondary chemical reactions due to operation and control limitations and reactions of impurities introduced with the materials. Therefore, the following relationships constrain the operation and productivity of the cells:

$$Q_{cell}\,(W) = V_{cell\ to\ cell} * I = V_{at\ cell} * I + I^2 * R_{external\ busbar} \quad \textbf{(EQ 5)}$$

where

$V_{cell\ to\ cell}$ = repetitive voltage between cells connected in series (typically between 4.0 and 4.6 V)
$V_{at\ cell}$ = voltage gradient between the anode beam and the cathode busbar
$R_{external\ busbar}$ = ohmic resistance of the cell-to-cell interconnection in busbars
I = current passing through each cell (while all are maintained constant in potline operation)

The energy introduced to the cell environment ($V_{at\ cell} * I$) needs to have an average energy input rate to satisfy the following general relationship because the materials are all introduced at room temperature:

$$V_{at\ cell} * I = Q_{preheat\ materials\ added} + Q_{all\ reactions} + Q_{heat\text{-}loss\ of\ cell} \quad \textbf{(EQ 6)}$$

The horizontal orientation of both anode and cathode means that the productivity per cell is low, with the largest cells (~600 kA) producing less than 4.6 t of aluminum per day, yet each of these cells requires an operating footprint of 100 m^2. Therefore, it is not surprising that the cell heat loss, $Q_{heat\text{-}loss\ of\ cell}$, accounts for approximately half the energy input.

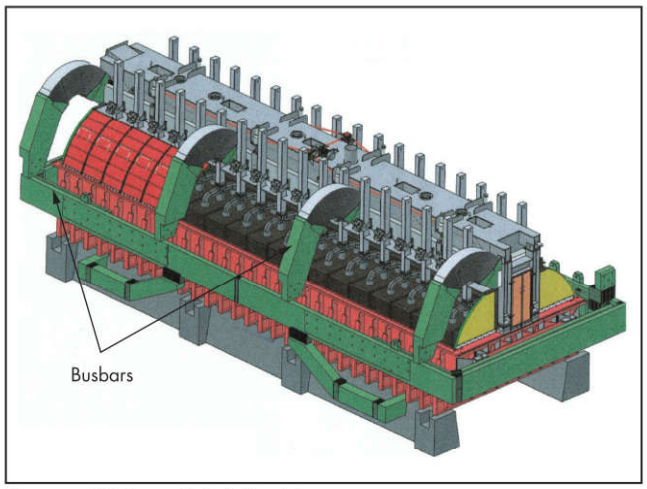

Courtesy of Emirates Global Aluminium

Figure 2 Computer-generated pre-construction design model of the DX+ cell technology of Emirates Global Aluminium, displaying the cell-to-cell interconnection with anode and cathode busbars

INDUSTRIAL POTLINES

Aluminum is a globally traded metal, so smelters are usually located close to a good transport system—often shipping—to enable the smelter to both receive the materials resources and deliver the product. However, as the user of an immense amount of electrical energy, the majority of operating smelters are also located a modest distance away from the primary source of electrical energy (such as hydroelectric dams). Consequently, the most efficient way of transmitting the energy to the smelter site is as AC at a high voltage. Commonly, it is also interconnected to a national grid for security of supply.

The AC power is converted to high-voltage DC power by rectifying transformers with efficiencies ranging from 97% to 98.5%. Because of the heat generated within the rectifier units, their current capacity is limited and usually several are interfaced in parallel to safely provide the necessary line current.

As illustrated in Figure 3, the cathode of one cell is electrically connected to the anode of the next cell to form a cell line (in industry jargon, it is called a *potline*). Series connection allows the use of high-voltage rectifier transformers with the rectified voltage, varying from 400 to 2,000 V DC. The number of cells interconnected in series is set to enable the potline to operate at a line voltage about 50 V below the supply design limit. This voltage constraint is to provide a reserve if any cell requires extra voltage due to process excursions, for starting newly reconstructed cells, or for other emergencies such as providing the extra heat when the line current has to be reduced through failures of rectiformers. Process excursions occur in an unpredicted manner when the alumina concentration of an individual cell is depleted to the extent that the electrochemical reactions at the anode change to include formation of perfluorocarbons, which form a resistive intermediate on the surface and the ohmic resistance can lift the cell voltage in excess of 20 V. Today, smelters interfaced to the national electricity distribution grid are expected to reduce their consumption to make energy available to the community, and this is done by reducing the line current, but, as evident from Equation 6, to maintain the cells at temperature, an increase in the voltage of each cell then becomes necessary.

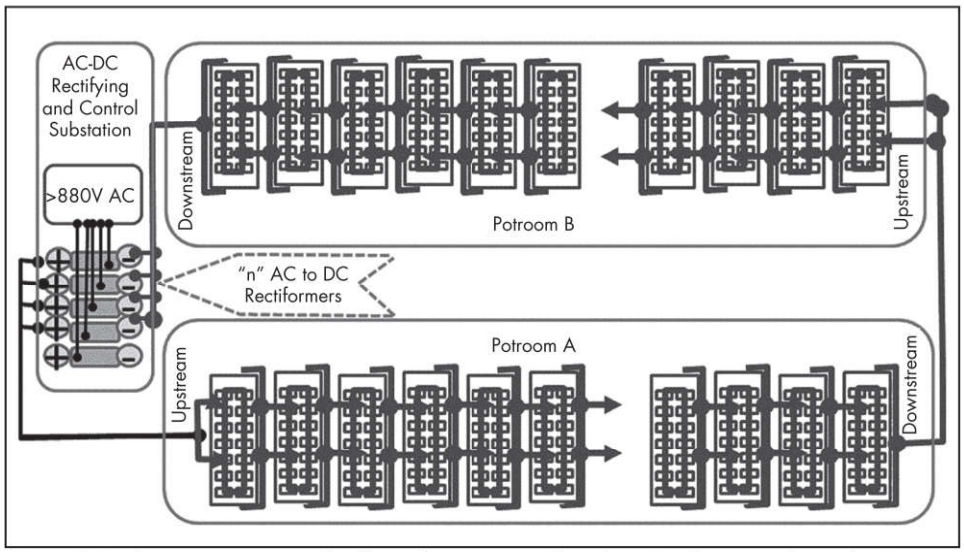

Figure 3 Basic arrangements of cells and power supply substation for a modern aluminum smelter

For many years, aluminum smelter potlines typically had about 200 cells in series (as a consequence of having 880-V supply available), split into two rooms to circumvent the need of a return busbar. More recently, potlines with up to 440 cells have been constructed. In the latter case, the line voltage can reach as high as 2,000 V DC.

Subject to satisfactory workspace and ventilation, the side-by-side cells are positioned as close as possible, with typical modern cell-to-cell spacing between 6 and 6.5 m, depending on design and technology.

The potline interconnection of cells in series is not without risk, as failure of one cell can interrupt the whole potline. Consequently, the cell design features include ways of rapidly bypassing an individual unit. Figure 3 also highlights two other common terms used in operations—the more positive side or end of a cell is referred to as being *upstream* while the more negative side or end is referred to as being *downstream*.

The DC power plant needs to meet requirements for supply reliability, because an interruption in power supply for more than a few hours will result in cooling of the electrolyte to the extent that it can totally freeze, losing its electrical conductivity, and thereafter it is not possible to pass current to restart the cell. In the intermediate time zone, the forces generated by partial freezing can also damage the carbonaceous and refractory materials of cell construction. All will result in serious problems to the aluminum production process. Power plant designs therefore include spare capacity in the form of rectifying transformer units, so the installed power plant is oversized for the smelter. This is called the n-1 principle and is illustrated in Figure 3, where it is noted that one of the rectifying transformers is not connected to the cell busbar network, although it can be readily cut into circuit if needed. It also has the advantage that, at any necessary time, a single unit can be cut out of service for routine maintenance and servicing. However, with the growing demand for the metal but variable supply of electrical energy from National Grids (which can include wind or solar energy), the spare rectifying transformer can also find intermittent use by increasing the current through the potline for a short term, thus utilizing energies that would otherwise be wasted for production of metal.

Courtesy of Norsk Hydro

Figure 4 Modern side-by-side 300+ kA cell line in Sunndalsøra, Norway

Because of the similarities in designs and materials of construction of each cell in the potline, they all tend to operate with voltages within ±50 mV of the average value, with most of the fluctuations being randomly distributed because of the work practices and control strategy. Accordingly, the total line voltage has little variability, and hence, the potline current tends to be constant. Today, power plants have stabilizing units to ensure that a constant potline current is maintained unless there is a failure of the equipment or an operational need to make variation. The modern side-by-side cell potline room shown in Figure 4 also highlights several other features that need to be incorporated in the design and construction of aluminum smelters.

In Figure 4, on the left-hand side of the building, a duct can be seen that is used to convey the emissions and cell gases

to a central collection and fume treatment plant so that there are minimal process emissions. Perhaps not surprisingly, this end of the cell is referred to as the duct end. For safety reasons, this duct is electrically insulated from the cells, but outside the building, they all go to a common duct. Collection fans are generating the reduced pressure necessary. The wide aisle on the right-hand side of the cell (referred to as the tap end) is for service vehicles such as replacement anode delivery, and the metal "tapping crucible" is used to vacuum-siphon the metal production from the cell. Overhead cranes are used for assisting these work practices and also for transporting "ore bins" filled with SGA for replenishing the supply in the cells storage hopper. However, modern smelter designs use enclosed air-assisted transport systems that maintain a reliable supply of the alumina at the cell and eliminate the spillage and dust generation inherent in the earlier alumina replenishment systems. The piping of such a modern alumina transport system is evident just to the right of the fumes duct.

In the right foreground of Figure 4, another service unit can be seen, this being the anode butt cooling station. When spent anodes are removed from the cell, they are at temperatures in excess of 900°C and coated with liquid and solid electrolyte, which can evolve fluoride vapors, and gaseous and particulate hydrolysis products from interaction with the moisture of the air. This cooling station enables used anode cooling and simultaneously captures the undesirable emissions.

NECESSARY MATERIALS AND SUPPORT SERVICES

Even though the potroom becomes the nerve center of aluminum production, aluminum smelters also require a continuing supply of DC electrical energy, and alumina. Support services are also required for the supply and removal of carbon electrodes and for transforming the metal siphoned from the cell to a deliverable product for customers. The metal treatment center is referred to as the cast house. Prior to 1960, almost all aluminum smelters extracted their own alumina from bauxite within their smelting complex, but most smelters now purchase the refined SGA from specialized refineries. Consequently, a modern aluminum smelter is usually comprised of the following sections:

- Storage facilities and transport systems for distributing the alumina to the cells
- Two or more potrooms with the cells interfaced in series—these potroom pairs are connected at one end to a stabilized DC power source
- A high-voltage AC power supply or nearby generation from natural gas, coal, or hydroelectric dam
- An anode production facility comprising a paste- and shape-forming unit (green carbon), baking facility, and "anode rodding room" for preparing the anodes for application in the cell
- A "tapped metal treatment station" for metal quality upgrade
- A cast house for product shape and chemical composition adjustment to produce the metal grades appropriate to the application
- A gas treatment center for recovery of volatiles and particulate emissions from the cell

Historically smelters have had a bad reputation for their impact on the environment, but today almost all the gaseous hydrogen fluoride emissions are captured in a "dry scrubber" (or fume treatment plant or gas treatment center) and recycled back to the cell. This is done by adsorption of the gaseous hydrogen fluoride on the SGA. Nevertheless, to achieve efficiency, the Brunauer–Emmett–Teller (BET) surface area and the phase structure of the alumina are compromised. This sequence of operating units, excluding the anode production and rodding, is integrated according to the flow sheet in Figure 5 of a modern aluminum smelter showing the basic range of products prepared for shipment to customers.

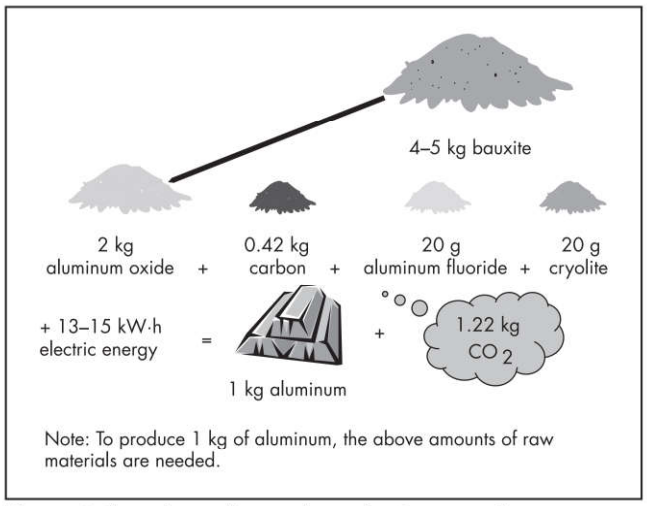

Figure 5 Flow sheet of a modern aluminum smelter

ENERGY RESOURCES

Although most of the earlier smelters were located within reasonable transmission range for electrical energy generated from the potential energy of hydroelectric dams, with a few exceptions, the global availability of such resources has been exhausted. Geopolitical or infrastructure resources mitigate against using the few remaining ones that are of sufficient size and located in regions where there is little demand from the human consumer sector. Consequently, there has been a gradual shift to using thermal energy conversion systems for the electrical energy supply.

Data for the mix of power sources for aluminum production in 2016, reported to the International Aluminium Institute (IAI 2017), show the percentages given in Table 3, including Chinese aluminum production.

Table 3 contrasts with a situation in 2000 when the industry was dominated by hydroelectricity generation, whereas coal is now the dominant resource for electrical energy used in aluminum production. This change has an important global environmental consequence because of the high carbon dioxide (CO_2) emissions from coal-fired power plants, many of which have a carbon footprint several times as high as the smelting process itself. However, the modern shift has been to use natural gas resources, which have a lower CO_2 footprint and higher thermal efficiencies. This is particularly so in the Middle East region where the lower-grade energy is also used successfully for producing potable water via desalination.

SMELTER-GRADE ALUMINA

In the electrowinning process, alumina is consumed according to the stoichiometric ratios given in Equations 2 or 3, leading to a theoretical consumption of 1.89 kg of Al_2O_3 per kg Al produced. However, in practice, the industrial value quoted is

Table 3 Four main sources of electric power for 2016 global aluminum production

Primary Energy Source	Percentage
Coal	61
Hydroelectric	27
Natural gas	10
Nuclear	1.5

Data from IAI 2017

Note: In Iceland, some thermal energy for aluminum production is extracted from geothermal resources while in China some 7% of the electrical energy used for smelters comes from wind power or solar panels.

usually in the range of 1.92 to 1.93 kg of Al_2O_3 per kg Al, the difference due to the impurities in the alumina, a feature often ignored in mass balance calculations.

Although the primary purpose of the alumina is to make aluminum in the smelting process, its properties must

- Be compatible with the alumina handling systems integrated into the smelter (such as the transport systems and volumetric point feeders used to dose alumina into the electrolyte);
- Enable the cell to make metal to the required purity and not introduce harmful alloying metals;
- Have a minimal amount of alkali and alkali earth elements, as these also accumulate in the electrolyte, harming the required physicochemical properties;
- Have adequate, assessable surface area to chemisorb the gaseous hydrogen fluoride released during the smelting process so that it can be returned to the process (as aluminum fluoride). This recovery process is referred to as dry scrubbing; and
- Also be used to both insulate the top of the anodes to conserve the heat and simultaneously prevent access of air to avoid unwanted oxidation of the hot carbon. Accordingly, there are a range of physicochemical properties that are sought by smelters, and these are usually encompassed in quality specifications, as shown in Figure 6.

The extensive range of properties listed in Figure 6 fall into the following five categories:

1. **Those pertinent to the dry scrubbing process and generation of emissions.** They include specific surface area or BET surface area, alpha content (the thermodynamically stable phase), and moisture content including monohydrate, $Al_2O_2(OH)_2$. During the dehydration and transition from the alumina trihydrate precipitated in the Bayer process to the finished product, various transition phases are formed, and these generate much of the surface area available for the adsorption of the gaseous hydrogen fluoride in the fume treatment process. However, this surface area is at the expense of having the residual $Al_2O_2(OH)_2$, which is typically present in the final product at levels of 4–5 mol %, and it has been demonstrated that the dissolved species generate much of the hydrogen fluoride that it is necessary to adsorb (Patterson 2002). Hence, there is often debate on the optimum specifications for this purpose.
2. **Handling properties, such as particle size and distribution, attrition index, angle of repose, and flowability.** Having high proportion of fine particles (less than ~45 μm) adversely affects the consistency of flow and transport properties, leading to irregularities in delivery via the transport system and inconsistencies in the volumetric mass discharged at each point feeder in the cell.

Certificate of Analysis—Alumina

Ship: _____ Shipment Date: _____

Description of Goods: Alumina in Bulk

Quantity Loaded: _____ t (metric tons)

1. Chemical Analysis

1.1	SiO_2	0.011	%	1.7	Ga_2O_3	0.009	%
1.2	Fe_2O_3	0.008	%	1.8	V_2O_5	<0.002	%
1.3	TiO_2	0.003	%	1.9	ZnO	<0.001	%
1.4	Na_2O	0.36	%	1.10	MnO	<0.001	%
1.5	CaO	0.014	%	1.11	K_2O	<0.002	%
1.6	P_2O_5	<0.0005	%				

2. Physical Analysis

2.1	Size		
	+100 mesh	12.2	%
	+200 mesh	71.9	%
	+325 mesh	92.8	%
	Superfines (–20 μm)	0.7	%
2.2	Flow time, 2 mm	3.7	minutes
2.3	Flow time, 4 mm	67.1	seconds
2.4	Surface area (BET)	81.4	m^2/g
2.5	Loss on ignition: 300°–1,000°C	0.92	%
2.6	Attrition index	19.1	%
2.7	Loose bulk density	1.000	g/cm^3
2.8	Angle of repose	29.7	°
2.9	Alpha alumina	2.9	%

Figure 6 A set of typical alumina specifications as a certificate of analysis

The superfines (arbitrarily defined as being less than 20 μm) can become airborne during the feeding process because of the high velocity of cell gases exiting the feeder hole. This leads to further inconsistencies. Hence, the greatest attention is usually devoted to the fines content when assessing the quality of the shipment.

3. **Chemical demand of the electrolyte.** This group includes impurities that are stable in the electrolyte and not reduced by the aluminum metal. The alkali and alkaline earth metal oxide groupings fall into this category. They tend to accumulate in the electrolyte by reacting with aluminum fluoride forming the respective metal fluorides.
   - An alumina with 5,000 ppm sodium oxide will require the addition of more than 20 kg of aluminum fluoride to the electrolyte for every ton of metal produced, with the resulting reaction product being a surplus of the cryolite electrolyte according to the following reaction:

$$3Na_2O + 4AlF_3 = 2Na_3AlF_6 + Al_2O_3 \quad \textbf{(EQ 7)}$$

   - Similarly, calcium oxide produces calcium fluoride that will be produced by the following reaction:

$$3CaO + 2AlF_3 = 3CaF_2 + Al_2O_3 \quad \textbf{(EQ 8)}$$

   - If the amount of CaO exceeds about 12% of the Na_2O, it will result in both an increase in CaF_2 concentration and an increase in the density of the electrolyte, sometimes even to the point where metal and electrolyte inversions could occur.
4. **Impurities that impact the metal quality.** This encompasses most other metal oxides and includes any oxide that is completely reduced by aluminum and alloys with it. Silicon and iron oxides represent the greatest amounts in most SGA.
5. **Impurities that impact cell performance.** Usually these impurities are only being partially reduced by aluminum and therefore able to undergo cycling oxidation and reduction processes within the cell, lowering the faradic efficiency. Phosphorous oxides are the ones of greatest concern.

In the majority of smelters in the world, prior to delivering the alumina to the smelting cells, it passes through a fume treatment plant to adsorb the hydrogen fluoride and capture the fine particulate matter emitted from the cell, and typically this increases the feeding requirements at the cell to approximately 1.98 kg of (impure) alumina per kilogram of aluminum produced. Subject to the primary alumina having a low attrition index, the dry scrubbing process does not modify the handling properties significantly.

ANODE CARBON

Calcined Petroleum Coke

On the basis of Equations 2 and 3, carbon is considered a raw material in aluminum production, because carbon is consumed by the anode reaction.

Typically, between 390 and 430 kg of carbon are used per ton of metal produced by a combination of the reactions according to Equations 2 and 3, as well as excesses through faradic efficiency losses and secondary reactions and processes. This consumption figure is referred to as the net carbon consumption. However, because of metal purity requirements, only between 70% and 80% of each anode introduced to the cell is consumed during that cycle. This leads to the gross anode consumption figure, which ranges between 500 and 600 kg/t, but the residual amount is subsequently recycled.

The fundamental requirement for any carbon to be used as an anode is that it must be of adequate purity and be able to conduct electrical energy, and thus be potentially graphitizable. Although there is no naturally occurring material that satisfies these requirements, the coke residue from petroleum refining satisfies these requirements because the original starting material is usually complex ring structured. However, it usually carries with it chemically bound sulfur and trace elements, including nickel and vanadium. The green coke residue remaining after crude oil is initially refined by heat treating in the distillation units at about 450°C, and 4 to 5 bar pressure has to be heat-treated further by calcining to temperatures in excess of 1,100°C, and preferably >1,300°C. This evolves residual volatile constituents and converts the structure to ordered and better-conducting graphitic crystallites.

The specifications presented in Table 4, show that some of the impurities carry through to the calcined product. Of these, sulfur, vanadium, and nickel are considered to be undesirable. The vanadium and nickel contents impact the metal quality, while the sulfur introduces another gaseous pollutant that requires treatment. Sodium is a proven catalyst for oxidation, leading to higher carbon consumption through secondary reactions, and, consequently, it is highly undesirable.

The broader specifications listed in Table 4 have emerged as a consequence of a growing shortage of low-sulfur coke and the unfortunate link between vanadium and sulfur contents.

The linkage between the sulfur and vanadium in calcined petroleum coke (CPC) is illustrated in Figure 7, which correlates a wide range of petroleum coke sources. This figure demonstrates a growing trend to higher vanadium content within the coke sources available.

Coal Tar Pitch

For application within the smelting cell, the CPC, together with the clean, recycled residual material from the previously used anode (butt), have to be bound into a solid, low-

Table 4 Typical specifications for impurities carry through to the calcined coke

Property	Maximum or Minimum	Typical Specification	Broader Specification
Moisture, %	Maximum	0.3	0.5
Ash, %	Maximum	0.3	0.5
Sulfur, %	Maximum	3.0	3.5
Vanadium, ppm	Maximum	350	500
Nickel, ppm	Maximum	250	300
Iron, ppm	Maximum	300	400
Calcium, ppm	Maximum	200	250
Silicon, ppm	Maximum	250	300
Sodium, ppm	Maximum	150	200
Real density, g/cc	Minimum	2.05	2.03
Vibrated bulk density (28 × 48 mesh = 0.3–0.6 mm)	Minimum	0.85	0.82
Particle size (+4 mesh = 4.75 mm)	Minimum	25	25
De-dust oil, %	Maximum	0.3	0.5

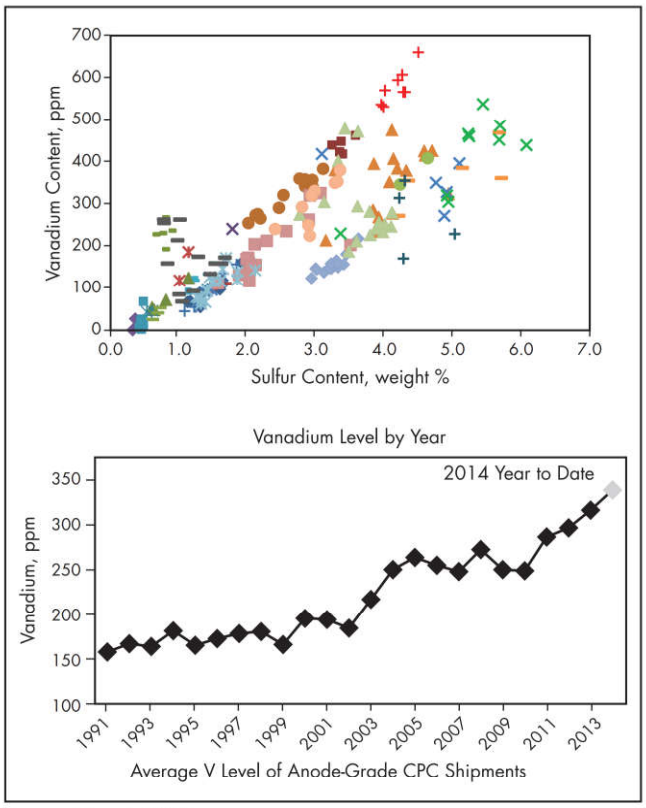

Source: Edwards 2015

Figure 7 Vanadium and sulfur contents in calcined petroleum coke shipments

porosity, compacted mass, and this introduces the requirement of a binder material.

The most satisfactory binder material for electrode production is coal tar pitch (CTP), the less-volatile components of the materials distilled from bituminous coking coals when producing coke for the iron and steel industry. Typically, carbon electrode production requires about one part by weight of pitch per six parts of CPC.

Softening point, viscosity versus temperature relationship, and coking value are all important properties sought in determining satisfactory CTP. The residual coke formed from the thermal decomposition of CTP should also assume a similar graphitic structure to CPC, and once heat-treated, it should have a similar reactivity.

THE ELECTROLYTE AND ITS OPTIMIZATION

The molten electrolyte in the cells has several important functions:

- To be the solvent for alumina to enable its electrolytic decomposition to produce aluminum at the cathode and carbon oxides at the anodes.
- To be a good ionic conductor for passing electricity from the anodes to the cathode in the cell.
- To provide a physical separation between the produced aluminum metal and the evolved carbon oxide gases to avoid the so-called back reaction.
- To provide a heat-generating resistor that enables the cell to be self-heating.
- To have an electrolyte with low enough density to cover and protect the metal from oxidation by the air.

In addition to these functions, it should be thermochemically more stable than the dissolved oxides in the environment (especially the reducing potential of aluminum and dissolved metal, and oxidizing potential of CO_2 gas) and electrochemical potential range applicable to the process at the electrode–electrolyte interfaces. This combination of requirements can only be satisfied by a selected group of molten fluorides.

The congruently melting cryolitic salts, K_3AlF_6, Na_3AlF_6, and Li_3AlF_6, all exhibit adequate solvency properties for alumina, and the resulting solutions all have melting points significantly above that of liquid aluminum. Of these, K_3AlF_6 dissolves the highest amount of alumina. Adequate but decreasing solubility of alumina is also exhibited if the alkali-fluoride-to-aluminum-fluoride molecular ratio is varied from the 3:1 proportions. Each of the cryolitic salts has a minor disadvantage linked with the fact that alkali metal has a small solubility in aluminum and co-deposits during the electrolysis process. The co-deposited alkali metal can be removed during subsequent metal treatment by a displacement reaction with pure aluminum fluoride. K_3AlF_6 has not found commercial applicability because the co-deposited potassium undergoes damaging secondary reactions with the electrode contact media, the graphitized carbon block that also serves as part of the container construction. This interaction causes a swelling and rapid deterioration of the carbon, limiting the cell life.

All alkali metals exhibit a significant solubility in their pure molten fluoride (Dworkin et al. 1962), with the solubility of potassium in molten KF exceeding 5 mol % at 850°C, and for Na in NaF it exceeds 2.5 mol % at 1,000°C. The co-deposited alkali metals also exhibit significant solubility in molten alkali fluorides, forming dissolved species that are readily oxidized if they come in contact with cell gases. This provides a mechanism for lowering the faradic efficiency for metal production. Again, of these, K_3AlF_6 is the worst, and the industry has standardized on using Na_3AlF_6 as the primary solvent component.

Electrolyte Maintenance

As seen from Equations 2 and 3, the electrolyte itself does not take a direct part in the main reactions for aluminum production. Fortunately, the solvent fluorides used to dissolve the alumina and other oxides present in the raw material are fluorides that are electrochemically more stable in the presence of a carbon anode under modest electrode potentials. There are a wide range of oxides that exhibit moderate solubility in the fluorides of their own salts, but salt melts containing the cryolitic anion AlF_6^{3-} formed from melts with the stoichiometric proportions of 3 alkali $F{\cdot}AlF_3$ have been found to exhibit the highest solubilities of alumina. After considering other properties, such as electrical conductivity of the resulting melt and the electrochemical tendency to co-deposit the alkali metal with the aluminum, cryolite (Na_3AlF_6) has become the solvent of choice, although occasionally blends of other alkali fluorides have been used.

The main losses of electrolyte occur through it penetrating into the porous materials of construction of the cell and gaseous or particulate fluorides not captured and recycled to the cell. Stringent environmental regulations exist that

typically limit the fluoride loss to less than 1 kg/t of metal produced. Leading-edge technologies have losses as low as 0.20 kg of fluoride per ton of metal.

Using Aluminum Fluoride as a Solvent Electrolyte Modifier

Tingle et al. (1981) demonstrated that the sodium solubility in cryolite could be reduced dramatically by increasing the excess aluminum fluoride content. The sodium content of aluminum in equilibrium with pure cryolite at 1,000°C is 175 ppm, whereas increasing the excess aluminum fluoride concentration to 11 wt % reduces it to less than 50 ppm. Given the following two interfacial equilibrium processes established in the NaF-AlF_3-Al, the sodium, and hence the dissolved metal solubility, are substantially reduced by this electrolyte modification:

$$3NaF\ (melt) + Al(l) \rightleftharpoons 3Na\ (in\ Al) + AlF_3\ (melt) \quad \textbf{(EQ 9)}$$

$$Na\ (Al) \rightleftharpoons Na\ (dissolved\ in\ electrolyte) \quad \textbf{(EQ 10)}$$

There has been speculation and model predictions in the literature that aluminum also dissolves as a subvalent species, but the reliable, detailed measurements of metal solubility that have been conducted have demonstrated that sodium is the prominent dissolved species for all electrolyte compositions, and, therefore, this equilibrium is sufficient for expressing the dissolved content.

Lithium Fluoride as an Electrolyte Modifier

Since lithium fluoride (LiF) is thermodynamically stable and gives rise to a small mobile cation and it is also stable within the cell environment, it has been introduced as an additive to the molten electrolyte to increase the electrical conductivity, thus enabling operating at a lower voltage for the same interelectrode distance. When introduced to the electrolyte (in the form of lithium carbonate), it forms lithium cryolite by reaction with excess aluminum fluoride. When LiF/Li_3AlF_6 is present in the molten salt system, it also lowers the melting point, with the beneficial effect of lowering the vapor pressure. These property changes were considered beneficial in some technology and electrolytes containing up to 3.5 wt % LiF were applied. However, the co-deposition of lithium, which can form the metastable Al_3Li phase (δ'), introduced problems for some of the applications of aluminum even though such precipitates strengthen the metal by impeding dislocation motion during deformation. With the advent of dry scrubbers for emissions control and the development of better cell alumina feed control, the disadvantages generally started outweighing the advantages, and lithium fluoride is now rarely used as a deliberate additive. However, some bauxite deposits have lithium oxide associated with them and this can carry through to the SGA. In such situations, a steady-state lithium fluoride concentration becomes established in the electrolyte—typically less than 1.5 wt % LiF equivalent. In the rare situations where it exceeds 2 wt %, it becomes necessary to treat the liquid metal to decompose the metastable Al_3Li phase.

Calcium Fluoride as an Electrolyte Modifier

In early development of the smelting process, many additives were tried to improve the electrolyte, especially to lower the operating temperature. These included magnesium and calcium fluorides, and calcium fluoride (CaF_2) was found to be beneficial for that purpose and became a common additive. However, there has never been any demonstration of other beneficial properties from calcium fluoride additions. The one harmful result is when the concentration exceeds approximately 7 wt %, the density of the electrolyte can increase sufficiently to risk metal/electrolyte inversions. It also reduces the alumina solubility. When this reaches a critical limit, its addition can be at the sacrifice of using aluminum fluoride, which has proven beneficial effects.

A commonly accepted compromise for these two additives is that the total weight percent of the two should not exceed 17. Therefore, many smelters have chosen 5 wt % CaF_2 as an ideal target. Depending on the quality of the Bayer processing and the bauxite mineral origin, oxides of sodium, calcium, lithium, and magnesium are sometimes present in the SGA, and consequently, these end up as fluorides within the melts, following reactions with regularly added aluminum fluoride, as illustrated in Equation 7. Simultaneously, cryolite is made by Equation 7 and in order for the concentration not to change significantly, the weight ratio of sodium oxide to calcium oxide in the alumina should be between 9 and 12. If the calcium oxide results in a lower ratio, extra electrolyte needs to be added to maintain the concentration.

Reducible Impurities

Both the anode carbon and alumina introduce trace amounts of other elements that are also transferred to the electrolyte via similar reactions to Equations 7 and 8. These include Ti, V, Be, Mg, Li, K, Ni, Si, Fe, and P. Initially, they are transferred to the electrolyte phase as a fluoride. If present in the anode, this could be electrochemically generated, for example:

$$4F^- + Si\ (anode) \Rightarrow SiF_4\ (electrolyte,\ at\ electrolyte–gas\ interface) \quad \textbf{(EQ 11)}$$

This generates a concentration in the electrolyte where two loss processes occur:

$$3SiF_4\ (in\ electrolyte) + 4Al(l) \rightleftharpoons 4AlF_3\ (in\ electrolyte) + 3Si\ (in\ Al) \quad \textbf{(EQ 12)}$$

and vaporization, at a rate proportional to its concentration:

$$SiF_4\ (in\ electrolyte) \rightleftharpoons SiF_4(g) \quad \textbf{(EQ 13)}$$

Most of the impurities listed either co-deposit or are virtually quantitatively reduced by the liquid aluminum degrading the metal quality. A few others are "partitioned" according to this exemplifying illustration. The less reducible impurities, such as the alkali and alkali earth impurities, accumulate as fluorides in the electrolyte.

Solvent Composition and Saturated Alumina Solubility

It is evident that the cryolite anion, AlF_6^{3-}, is essential for dissolution of the alumina, with it dissolving by a chemical reaction that can proceed to equilibrium. Many reactions have been proposed, including the following:

$$Na_3AlF_6 + Al_2O_3 \rightleftharpoons 3NaAlOF_2 \quad \textbf{(EQ 14)}$$

$$2Na_3AlF_6 + 2Al_2O_3 \rightleftharpoons 3Na_2Al_2O_2F_4 \quad \textbf{(EQ 15)}$$

$$4Na_3AlF_6 + Al_2O_3 \rightleftharpoons 3Na_2Al_2OF_6 + 6NaF \quad \textbf{(EQ 16)}$$

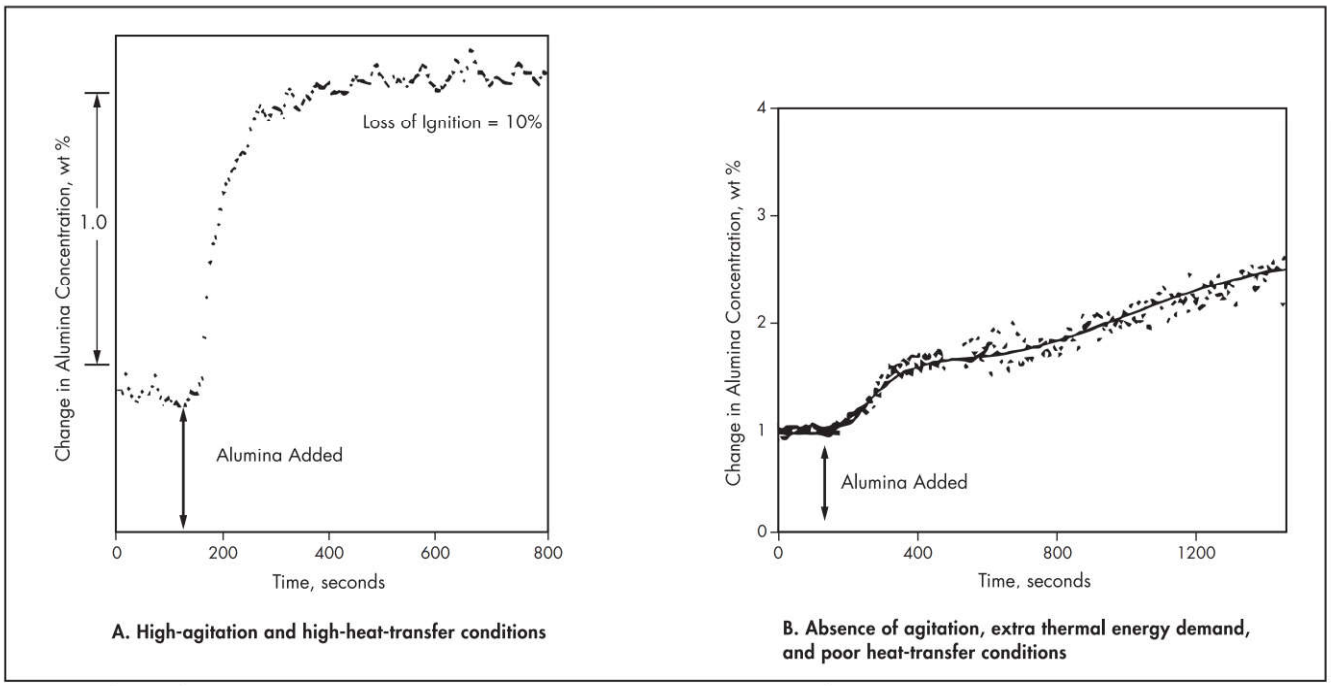

Source: Bagshaw et al. 1985 Source: Jain et al. 1983

Figure 8 Differences in alumina dissolution and mixing in an electrolyte

Key features that arise from various studies include the fact that dissolution is very endothermic, with a heat of dissolution exceeding 108 kJ/mol, and the cryolite anion AlF_6^{3-} concentration in the melt limits the alumina solubility.

Alumina Dissolution Kinetics and Mixing

Specifying conditions for adequate dissolution kinetics is like writing a dissertation on the optimum way of sweetening one's coffee by adding sugar. We know qualitatively how it is achieved: not adding too much, adding it in a powder form, coupled with rapid agitation to disburse, and having a hot solvent. We also know that if it is not done correctly, it does not all dissolve and forms a residue in the bottom of the cup, despite not having exceeded the saturation solubility.

The endothermic dissolution of alumina has many parallels, but it has two added complications. The first is the powder added is cold (near room temperature), and basically, this doubles the energy requirements for dissolution. The second is that because of the cell design and materials of construction, the operating temperature of the electrolyte should be controlled near its liquidus point (<15°C), so we potentially have the situation analogous to dipping the ice cream in hot chocolate—a protective coating is formed on addition. Practically, therefore, heat transfer becomes an important consideration. The significance of this cannot be underestimated, because essentially, each kilogram of primary alumina added requires more than 0.54 kW·h/kg to achieve preheat and dissolution. If this were achieved by extracting from 10 kg of electrolyte, it would need to lower the superheat by 10°C and simultaneously freeze one-third of the electrolyte mass.

The aluminum smelting industry has been concerned about dissolution kinetics because of the need for maintaining a minimum concentration to sustain the electrochemical processes, and also to prevent the formation of a resistive layer of undissolved alumina underneath the metal pad and thus disrupting uniform current flow. Although the results and interpretation of many of the investigations in laboratories for the dissolution kinetics of alumina are often a consequence of the experimental design, several general trends have been confirmed from detailed analysis of published results. These include the following:

- At low superheat of the electrolyte, the process is controlled by heat transfer.
- The dissolution speed is retarded for electrolytes using high excess aluminum fluoride concentration.
- SGA that releases volatiles on addition tends to disperse better in the electrolyte and have faster dissolution kinetics.
- Agitation has a similar impact.
- The dissolution rate is reduced as the electrolyte approaches saturation.

The two dissolution curves shown in Figure 8 illustrate the extremes with the dissolution times for an addition that should increase the concentration by ~1.0 wt %. It ranges from less than 20 seconds to more than 10 minutes when the superheat is low and there is an absence of agitation (Bagshaw et al. 1985; Jain et al. 1983).

All the observations and measurements of the dissolution kinetics are consistent with standard interfacial heat and mass transfer controlled processes, with the speed decreasing as the concentration of the cryolite anion is reduced (hence, the aluminum fluoride concentration impact) or as the interface achieves its equilibrium saturation value. And it is increasing as the interfacial contact area (through dispersion or agitation) is increased. Therefore, the following generalized mass transfer rate equation is useful for describing the process, regardless of whether it is mass or heat transfer controlled:

$$\text{rate } Al_2O_3 \text{ dissolving} = k_{m/h}\cdot(\text{area in contact})\,[Na_3AlF_6\ (\text{liquid})]^n \cdot[C_{Al_2O_3,\ \text{saturated}} - C_{Al_2O_3,\ \text{bulk electrolyte}}] \quad \textbf{(EQ 17)}$$

where the applicable heat or mass transfer rate constant, $k_{m/h}$, is used, and while the order of the dependence of concentration of the cryolite anion, "n", represents the inadequately determined order for the cryolite concentration influence. Moving to electrolytes using ~11 wt % excess aluminum fluoride became dependent on developing point feeders so that alumina concentration, dissolution kinetics, and mixing could be optimized.

Prior to the development of point feeders, massive additions of alumina were made to the cell—amounts ranging from 50 to 250 kg per addition; therefore, having a high solubility of alumina was crucial, even though undissolved alumina would invariably be found within the cell. Subsequently, the shift to small addition as typified by point feeders, and the development of low alumina concentration sensing feeding logic, enabled operation of the cells at lower concentrations under normal conditions while ensuring good alumina solubility. This facilitated a shift away from the cryolite stoichiometry on the aluminum fluoride–rich side of the phase diagram to reduce the metal solubility in the electrolyte and thus raise the faradic efficiency of the cells. Consequently, between 1960 and 1990, the trend in the industry was to gradually increase the AlF_3 concentration in the electrolyte from about 3 wt % up to the level of 10–12 wt % that is used now.

Operating Temperature and Electrolyte Maintenance

The liquidus temperature of the modern point-fed electrolyte is typically in the band 942° to 955°C. For operational and cell life reasons, it is usually desirable that the operating temperature be no more than a few degrees above the liquidus temperature to ensure retention of a frozen cryolite layer around the sidewalls. This layer acts as a thermostat (through freezing or melting if there is transient imbalance in the energy content of the electrolyte) and also forms a leak protection barrier while preventing undesirable horizontal current flow between the end of the metal pad and the otherwise electrically conducting sidewall components.

Consequently, the operating temperature should be between 955° and 965°C. This temperature and composition band also ensure that the density of the electrolyte remains within the band of approximately 2.08 to 2.12 kg/dm^3 (compared to 2.30 kg/dm^3 for the molten metal), ensuring that liquid inversion is avoided in the normal stability range of the liquid aluminum metal pad.

The total mass of electrolyte used in the cell varies with design, which particularly influences the free volume between the electrodes and the sidewalls of the cell. During the last 50 years, the average cell size of the leading-edge technologies has increased dramatically, with the operating line current typically being three times that of the first generation of mechanically fed cells. Through extensive mathematical modeling of the impact of the magnetic field on the metal pad, design variations have also reduced the distortion of the metal surface as well as lowering the metal pad velocity, thus enabling operation at reduced interelectrode distance—the zone occupied much of the electrolyte. Simultaneously, to maximize productivity, the size of the anodes has been increased within the cell by reducing the surrounding free volume presented by the gaps between each anode block and the gap at both the center channel and between the outer edge and the cell sidewall. Consequently, the mass of electrolyte per cell kiloamps has been reduced quite dramatically.

The steady reduction in electrolyte mass per kiloamp tightens the requirements for alumina dissolution and mixing, and accordingly, the control of the chemical composition of the electrolyte is also of greater importance.

ELECTROLYTE COMPOSITION CONTROL

The composition of the electrolyte is selected for optimum overall cell performance; therefore, smelters generally take routine samples of the electrolyte for analysis so that corrective actions can be taken to adjust the composition to the target control band. While there have been a range of sensors developed to assist solvent composition control, the impact of the operating dynamics plus limited accuracies of the sensors generally result in limited sampling for analysis of individual cells by a laboratory with resulting slow feedback. Although the solvent electrolyte is fairly inert to the primary electrochemical processes, losses of electrolyte components occur through secondary processes within the cell, as summarized later in Table 6. For example, cells typically emit about 20 kg of hydrogen fluoride for every ton of aluminum produced, although the amount of this is dependent on the climate and quality of alumina used and can vary by 50%. Most of the hydrolyzing material originates from moisture or structural water introduced by the alumina. Component losses also occur through vaporization, with the main volatile component being sodium tetrafluoroaluminate ($NaAlF_4$). More than 95% of these emissions are captured and recycled back to smelting cells, with each cell receiving the average amount lost rather than the amount lost through its individual process conditions prevailing. Consequently, limited variation for individual cells can occur through these mechanisms.

The components of the electrolyte derived from aluminum fluoride also become the dominant variable, normally requiring replenishment. This is because of its reaction with the alkali and alkaline earth metal oxides present in the SGA to form stable fluorides, as illustrated by Equations 7 and 8. As seen in Table 5, the amount of these oxides can vary considerably. The amount of aluminum fluoride necessary is greater than given by Equations 7 and 8 because an additional amount is needed to readjust the newly formed cryolite to the target proportions. A simple material balance correlation for the amount of aluminum fluoride consumed by the electrochemically stable SGA impurities is given by the following equation:

$$\text{kg } AlF_3/\text{ton Al} = 34.3\cdot[\%Na_2O] + 19\cdot[\%CaO] + 0.49\cdot[\%Na_2O]\cdot[\%AlF_3] \quad \textbf{(EQ 18)}$$

where the percentages of the oxides are based on weight, as is the percentage of excess aluminum fluoride above the stoichiometric cryolite composition.

The AlF_3 maintenance needs for "new cells" (i.e., less than a year old) are invariably less than predicted by Equation 18, and it can even be nonexistent in the first 60 days of operation. This is a consequence of the carbonaceous material used for the cathode lining that takes up a large amount of sodium, forming sodium–carbon intercalation compounds until localized saturation at the interfaces is reached. The source of the sodium is from either direct electrodeposition or via co-deposition with the aluminum. However, Equation 18 serves

Table 5 Thermodynamic analysis of the electrochemical reactions established in smelting cells (based on thermochemical database)

Important Electrochemical Reactions Occurring in the Cell	Equation No.	$\Delta H^\circ_{reaction}$, kJ	$\Delta G^\circ_{reaction}$, kJ	$E^\circ_{enabling}$, V	$E^\circ_{revised\ estimate}$, V ±0.04	$E^\circ_{complete}$, V
Normal Metal Production						
$Al_2O_3 + 3C = 2Al + 3CO(g)$	2	1,351	622	1.074	1.10	2.333
$Al_2O_3 + 1.5C = 2Al + 1.5CO_2(g)$	3	1,099	690	1.191	1.22	1.898
$Al_2O_3 + 3C + 3S = 2Al + 3COS(g)$	19	1,203	568	0.980	1.03	2.103
Generation of Gaseous Emissions						
$1.5Al_2O_3{\cdot}H_2O + Na_3AlF_6(l) + 3C = 4Al + 3HF(g) + 3CO_2(g) + 3NaF(l)$	4	2,617	1,239	1.041	1.07	2.644
Perfluorocarbon Formation Initiation Reaction						
$Al_2O_3 + 3C + 2Na_3AlF_6(l) = 4Al + 3COF_2(g) + 6NaF(l)$	20	2,877	2,157	1.863		2.485
$Al_2O_3(s) + 4.5C + 2Na_3AlF_6(l) = 4Al + 3CO(g) + 1.5CF_4(g) + 6NaF(l)$	21	3,061	2,085	(1.811)	1.85	2.644
$4Na_3AlF_6 + 3C = 4Al(l) + 12NaF + 3CF_4(g)$	22	3,496	2,986	2.578		3.020
$2Na_3AlF_6 + 2C = 2Al(l) + 6NaF + C_2F_6(g)$	23	1,813	1,618	2.796		3.132

as an excellent predictor of the aluminum fluoride demand for mature cell operation.

Since the sodium oxide content of the SGA from almost all alumina refineries normally exceeds 0.3 wt %, the demand justifies installing an aluminum fluoride feeder that adds aliquots in controllable proportions to help maintain the target concentration band. Thereafter, limited variations are made based on cell condition variations and sample analysis. A range of predictive algorithms exist for estimating the aluminum fluoride additions required. The predictive challenge arises because of the lack of knowledge of how much of the frozen side ledge—which is more than 97% pure cryolite—has transferred into or out of the electrolyte through small temperature fluctuations, or what the actual liquid electrolyte mass or volume actually is.

Electrolyte Mass Control

Varying and unpredictable electrolyte losses can also occur as a consequence of the anode change and metal tapping work practices, and these losses occur into crack openings in the cell lining and create leakages into the insulating material below. In the opposite direction, if the sodium oxide content exceeds 0.3 wt %, usually the cells become electrolyte producers because of the amount of aluminum fluoride being added. A typical common feature linked to the mass of the electrolyte is the total electrolyte depth in the cell, and this becomes the control measure for the mass of electrolyte in the cell. The depth is determined by dipping a steel rod into the electrolyte and metal pad and, after a short time (typically 5–10 seconds), removing it and measuring the length of frozen electrolyte on the rod. Because of differences in heat and mass transfer in the metal pad, there is an identifiable step in the thickness of the frozen layer at and below the metal pad surface. Typically, operating technologies target a depth between 15 and 20 cm, but because of the limited accuracy of measurements, the electrolyte depth control usually has a 2-cm control band. The height variation only affects a limited mass because about 80% of the electrolyte is in the planar surface underneath the anodes.

The source of the electrolyte material, when needed, is usually from another cell because of the tendency to overproduce electrolyte. Depth maintenance is important for keeping the true current density constant, and this is important for controlling electrode reactions.

Electrochemical and Chemical Reactions Occurring in the Cell

During normal operation of aluminum smelting cells, the cathode product is a sodium–aluminum alloy with the sodium content varying between approximately 50 and 200 ppm, depending on process conditions. The alloy is also contaminated with impurities that are present in the anode or in the SGA and whose oxides can be reduced by the reaction with aluminum at the metal pad interface. While acknowledging that impurities could be electrodeposited, their amounts, as well as the amount of sodium co-deposited, is very small and insufficient to influence the potential of the cathodic electrode. Accordingly, it is common to assume there is only one cathode reaction, namely, the reduction of the aluminum ions from the electrolyte solution to form aluminum. Consequently, it is common in the literature to set the potential of the cathode reaction at 0 V and look at the combined electrode potentials as representative of the anode reaction potential. This is the equivalent of the normal hydrogen electrode in aqueous electrochemical systems. Therefore, in the subsequent discussion, the calculated potentials are generally assigned to the anode process.

A more diverse range of gaseous products have been evolved and identified at the anode with the proportions of different gases varying with operating conditions. The identified anode gases that have evolved include hydrogen fluoride (HF), carbon monoxide (CO), CO_2, carbonyl fluoride (COF_2), carbonyl sulfide (COS), carbon tetrafluoride (CF_4), and dicarbon hexafluoride (C_2F_6). Although all of them have some undesirable property environmentally, carbon dioxide is the most desirable one because it leads to a minimum amount of greenhouse gas emissions and forms an important part of the life-cycle chain. Consequently, the challenge in operating the smelting cell is to minimize the formation of the less desirable products by control of electrode potentials or other conditions.

While there is a range of potential constituents for giving rise to these reactions and the specifications for the raw materials, the series of unique chemical and electrochemical reactions that can form these products is presented in Table 5. This

table also includes the predicted change in standard enthalpy and Gibbs energies of each reaction at 960°C. In Table 5 the standard state selected for alumina is the saturated solution, so that data for pure solid alpha alumina can be used. The reacting fluoride components Na_3AlF_6(l) and NaF(l) have been selected because they have reliable thermochemical databases. Although all the reactants will be at a reduced thermodynamic activity, the selected reactants would be at the higher concentrations based on the Temkin model for molten salts. Accordingly, the standard-state values should be a close representation of the applicable ones in normal smelting electrolytes. However, adjustments are made using published activity models to minimize errors in enabling electrode potentials. In this electrowinning process, since products are not normally present and therefore reversibility cannot be established, the potential calculated from given energy is referred to as an enabling one.

For electrochemical reactions to proceed in a cell operating essentially at 1 bar pressure, the following three conditions must be satisfied:

1. The magnitude of the interfacial potential gradient at the electrode *must exceed* that predicted from the Gibbs energy for the reaction to achieve reversible conditions according to the following relationship:

$$E_{reversible} = -\Delta G_{reaction}/zF \quad \textbf{(EQ 24)}$$

where
z = number of electrons transferred per g·mole of reacting species
F = Faraday's proportionality constant

2. A favorable reaction mechanism must exist, combined with an increase in the electrode potential gradient, to maintain the kinetics (current density) of the reactions to be displaced from reversibility. This increase in electrode potential is usually referred to as overpotential or polarization.
3. The total energy transferring across the reacting interface must satisfy the enthalpy of the following reaction:

$$\Delta H_{reaction} = \Delta G_{reaction} + T\Delta S_{reaction} \quad \textbf{(EQ 25)}$$

The extra entropic energy $T\Delta S_{reaction}$ is often overlooked in thermodynamic predictions of energy requirements for this and alternative processes. The entropic energy can be provided by the electrode overpotential, but if this is insufficient, it must be supplied by heat transfer. In the aluminum electrowinning process, ultimately, the energy comes from the voltage. For this reason, the Gibbs and enthalpy energies are converted to equivalent voltages in the last two columns of Table 5. Comparing the last two columns of voltages highlights how the cell anode reactions can transgress to co-evolution of perfluorocarbons, since the enabling potential gradients (calculated from the Gibbs energy) can be exceeded before sufficient energy is provided by the total electrode potential necessary to complete the production of carbon oxides evolutions without extra heat transfer.

THE CATHODIC METAL DEPOSITION REACTIONS

Of the three cations present in the electrolyte, the deposition of aluminum has the lowest potential, and calcium requires the largest (more negative) potential gradient for deposition. Although the sodium cation is more stable, it will co-deposit in the parts-per-million region, typically forming solutions with between 50 and 200 ppm sodium. The reference equilibrium value (no electrolysis) for an electrolyte at 960°C and the equivalent excess aluminum fluoride concentration of 10.5 wt % is 50 ppm Na in Al, whereas a pure cryolite electrolyte with no excess aluminum fluoride at 1,000°C has 170 ppm Na in Al.

Expressing the respective aluminum and sodium deposition reactions in terms of the species present in the highest concentration according to Table 6 produces two respective deposition reactions:

$$AlF_6^{3-} + 3e^- \Rightarrow Al + 6F^- \quad \textbf{(EQ 26)}$$

$$Na^+ + e^- \Rightarrow Na \text{ (in Al)} \quad \textbf{(EQ 27)}$$

The respective deposition potentials at zero current will be

$$E_{(AlF_6^{3-}/Al)} = E^\circ_{(AlF_6^{3-}/Al)} - [RT/3F] \cdot \ln a_{Al} + [RT/3F] \cdot \ln (a_{AlF6}{}^{3-}/(a_F{}^-)^6) \quad \textbf{(EQ 28)}$$

and

$$E_{(Na^+/Na \text{ in } Al)} = E^\circ_{(Na^+/Na \text{ in } Al)} - [RT/F] \cdot \ln X_{(Na^+/Na \text{ in } Al)} + [RT/F] \cdot \ln (a_{Na}{}^+/(\Upsilon_{(Na^+/Na \text{ in } Al)})) \quad \textbf{(EQ 29)}$$

where
a_i = respective thermodynamic activities of the species, expressed as molecular or ionic fractions
X = mol fractions
Υ_{Na^+} = activity coefficient of the sodium in aluminum

However, the two metal deposition potentials at zero current must be equal, and they also have been arbitrarily set at zero:

$$E_{(AlF_6^{3-}/Al)} = E_{(Na^+/Na \text{ in } Al)} = 0 \quad \textbf{(EQ 30)}$$

For a cell under electrolysis conditions, the cathode will be subject to polarization, and the potentials of each of the reactions will shift by the same amount. Since the sodium dissolved in aluminum is in a very dilute solution, Henry's law will apply and the activity coefficient of the sodium dissolved in the aluminum will be constant. Hence, during electrolysis:

$$\eta_{\text{cathode at } i = i} = E_{(Na^+/Na \text{ in } Al)}\, i = i - E_{(Na^+/Na \text{ in } Al)}\, i = 0 \quad \textbf{(EQ 31)}$$

and therefore applying Equation 28 to these two scenarios produces the following equation:

$$\eta_{\text{cathode at } i = i} \cong [RT/F] \cdot \ln (X_{(Na^+/Na \text{ in } Al)}\, i = i/X_{(Na^+/Na \text{ in } Al)}\, i = 0)) \quad \textbf{(EQ 32)}$$

where $\eta_{cathode}$ is the cathode overpotential and because of the reference potential equal to the cathode potential as a consequence of the operating current density and cell conditions.

The sodium cation is present in the highest concentration and the ionic fractions of the species will not change substantially in the operating cell because of the controlled electrolyte composition. Therefore, the cathode polarization is readily given by the change in the sodium content of the aluminum produced. Based on the measured sodium analysis in the aluminum for various operating conditions, it is evident that the cathode polarization will seldom, if ever, exceed –150 mV. Consequently, a value of –100 mV has been allowed for the cathode potential in all thermochemical calculations.

Table 6 Energy required to sustain the chemical and electrochemical processes occurring in an aluminum smelting cell

	Pure Materials; Stoichiometric CO_2 as the Only Electrochemical Product		Typical Materials and Performance	
	kW·h/kg Al	kJ/mol Al_2O_3	kW·h/kg Al	kJ/mol Al_2O_3
Preheat materials	0.67	130	0.79	154
Conversion reactions	5.67	1,097	5.815	1,130
Performance band	0	0	±0.075	±15
Total process	6.34	1,227	6.605	1,284
Equivalent voltage needed, V	2.128	±0.050	2.216	±0.050

The sodium cation is also the smallest ion present in the solution, and there is no evidence of any tendency for it to form complexes. Therefore, it is not surprising that research has shown that the sodium cations are the dominating species for transporting electric charge through the electrolyte, and this results in a buildup of sodium ion concentration on the electrolyte side of the electrode potential gradient for metal deposition. In some operating technologies, this has been so great that it changes the liquidus temperature to the point that a photographic recording has been made of a thin layer of pure cryolite crystallizing on the metal pad surface. This is expected to occur before the sodium concentration in the metal becomes 180 ppm Na in Al based on the equilibrium data of Tingle et al. (1981).

GENERAL ISSUES OF ANODIC REACTIONS

There are two major differences at the anode:

1. The anode is consumed, and therefore all constituents within the anodic electrode undergo a process change.
2. All electrode products that leave the electrode surface in the gaseous state require significant entropic energy for the phase change for the final transformation. The transformation energy is supplied by the interfacial electrode potential and, if in deficit, it is based on the overall enthalpy of reaction supplied by heat transfer from the electrolyte.

A major consequence of the second point, as is evident by the equivalent potentials listed in Table 5, is that other reactions become enabled before the energy requirements can be satisfied by the electrode potential gradient alone; therefore, competitive mechanisms of parallel reactions can occur. The conductive heat loss through the anode provides competition for supplying the deficit in energy. For an average age anode, the required conductive heat loss across the interface approaches 10 kW/m^2.

Because of the interaction with the anode material, all anode reactions are heterogeneous, and therefore, other than the charge transfer step, the reaction rate control can be controlled by normal heterogeneous kinetic factors. These include surface coverage and interfacial concentrations as well as being subject to the energy supply to provide the total enthalpy.

Electrochemical Formation of Carbon Oxides

As seen in Table 6, there are two possible cell reactions, both of which involve the same anion source. Based on the thermodynamic data CO(g), formation is enabled at a lower interfacial anode potential than CO_2(g). But there is the unique dichotomy that, once the current density raises the anode potential above that enabling CO_2(g) formation, the total energy required for the product is much less.

During normal electrolysis of an aluminum smelting cell, which is usually at a current density between 0.7 and 0.9 $A \cdot cm^{-2}$, the carbon dioxide content of the anode gas exceeds that of carbon monoxide by a factor of between 3 and 5.5. However, some of the carbon monoxide can arise through secondary reactions, such as oxidation of the metal dissolved in the electrolyte, leading to current efficiency losses, or direct chemical reaction between carbon dioxide and the anode carbon according to the following equation:

$$C(s) + CO_2(g) \rightleftharpoons 2CO(g) \quad \textbf{(EQ 33)}$$

which, while being endothermic ($\Delta H°_{960C}$ = 168 kJ/mol CO_2), has a favorable standard Gibbs energy change ($\Delta G°_{960C}$ = –45 kJ/mol CO_2) that would result in the reverse gas composition ratios to those observed.

The interaction between the electrochemically evolved CO_2(g) with the anode carbon in the pores and emergent surface of the anode according to Equation 33 changes the net reaction for more of the metal; effectively it is being produced by carbon monoxide rather than carbon dioxide. This reaction can be minimized during the anode production process by maximizing the density (hence, minimizing porosity) and increasing the heat treatment or baking temperature to reduce the reactivity of the carbon.

Simplifications in teaching have led to the general interpretation that CO_2(g) is the "primary product" with carbon monoxide formation being kinetically inhibited. Based on this understanding, the literature quotes the theoretical carbon consumption as being 0.333 kg C per kg Al produced.

Such a concept is extremely questionable, however, since both gases originate from the same ionic species in the electrolyte, and both electrochemical reactions would involve similar surface intermediate products. It is also contrary to numerous research findings, such as the fact that the proportion of CO(g) evolved during electrolysis increases as the current density is reduced under design conditions that minimize carbon monoxide formation by a chemical reaction (Hume et al. 1992).

The mechanistic interpretation of reactions has been based on fitting conceptual mechanisms to Tafel curves obtained in laboratory measurements of anode interfacial potential changes as a function of current density (i.e., overpotential). Three sets of published data are presented in Figure 9 and they show an inflection indicative of two electrode processes. Although not shown here, Richards and Welch (1964) found that the curves showed a hysteresis, with the inflection between the two processes being minimized when the polarization curve is obtained by reducing current from a high value, and the electrode has been subjected to electrolysis. A fourth set of data that is not reproduced here but is the one on which most of the interpretation against electrochemical formation of CO(g) is based, is consistent with the illustrated data below 0.03 $A \cdot cm^{-2}$ and also above 0.4 $A \cdot cm^{-2}$ but is totally devoid of data at current densities between these points.

Each of these sets of data is consistent with two electrochemical processes as proposed by Dewing and van der Kouwe (1975), with each reaction displaying fast charge transfer but with the tendency to develop some form of

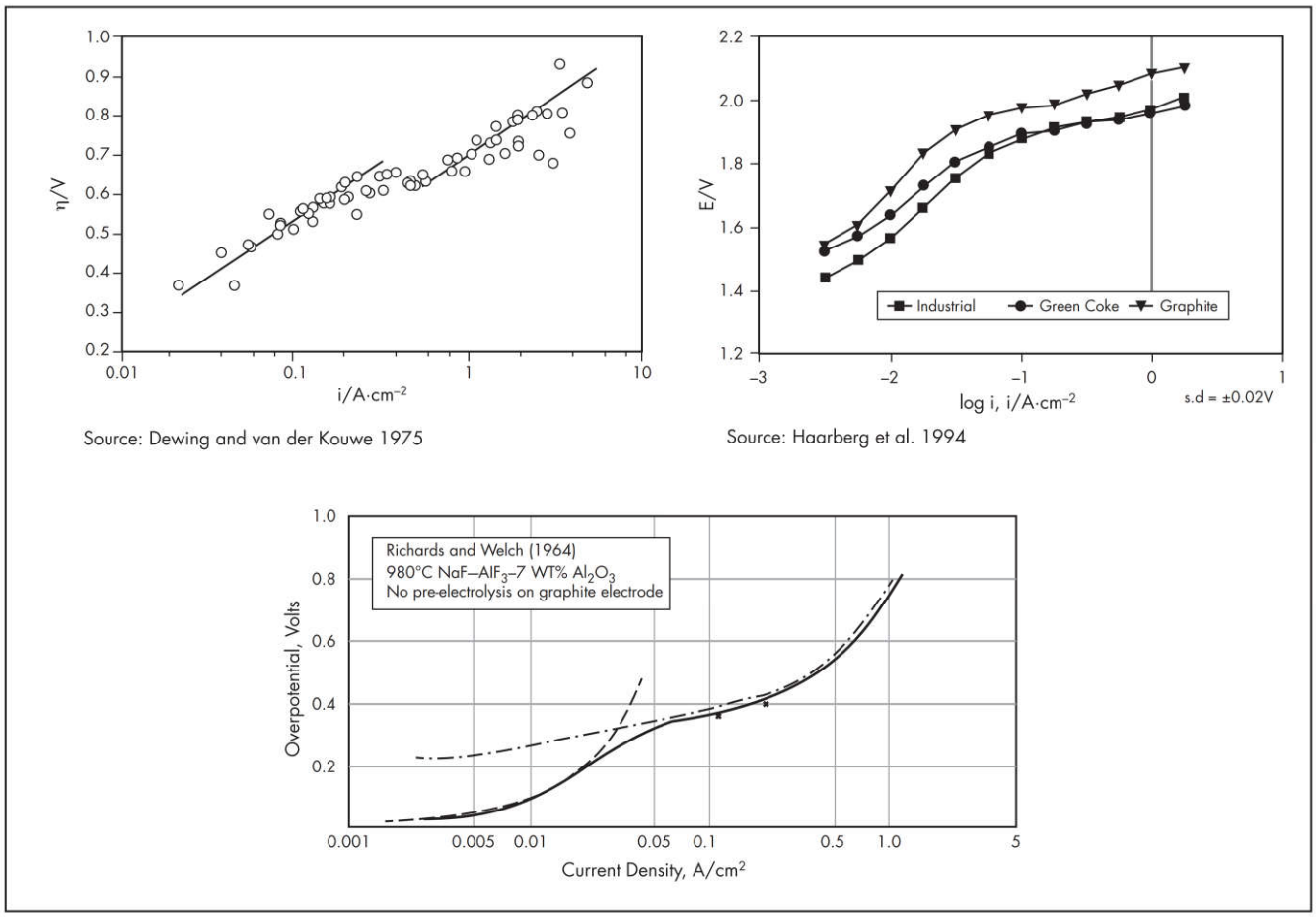

Figure 9 Comparison of three published sets of anode polarization which all have curves indicating a change in the electrode process while in the carbon oxide formation electrode potential region

concentration polarization. In the case of the first process, the formation of CO(g), the polarization would arise from surface coverage of the carbon anode, reducing the number of available sites for further discharge. It is extremely unlikely that it would be due to depletion of the oxide ions since they are involved in CO_2(g) formation as well. Such an interpretation would theoretically conform to the two superimposed (dashed) curves that have been annotated on the data graph of Richards and Welch (1964). However, for the first electrode process, since the same oxide anion is also involved in the second process, the concentration polarization is more likely due to buildup and surface coverage of a reaction intermediate on the carbon electrode. Furthermore, the Tafel slope and the shape of the polarization curve change once the electrode potential has increased enough to enable CO_2(g) formation. This is mechanistically consistent with the electrode polarization at high current densities being due to depletion of the oxide concentration, which is well known. However, one cannot eliminate a parallel contribution to the magnitude of the polarization being from surface coverage/concentration buildup of the reaction intermediate.

The existence of stable surface intermediates is supported by the dangerous back electromotive force that exists in operating cells that have been disconnected from their normal electrolysis power supply and are in the open-circuit mode. There have been observations of "residual gas evolution" continuing for a short time afterward as well. All research that has encompassed a range of different carbon structures for the anode (by heat treatment or graphitization) has found that the polarization—particularly of the first electrode process—is less with the more disordered carbon structure, and the proportion of carbon monoxide then increases.

Transitions from CO(g) formation at low current densities in the range 0.02 to 0.05 A·cm^{-2} to co-evolution of CO_2(g) at higher current densities is not only consistent with practical observations and carbon consumption data but also mechanistically explicable.

Electrochemical Formation of CO(g)

For modern operating current densities and slotted anode designs, between 4% and 8% of the current is being carried by electrochemical formation of carbon monoxide.

The most consistent mechanistic sequence of reactions would be as follows:

1. Local interfacial equilibrium dissociation:

$$AlOF_2^- + 2F^- \rightleftharpoons AlF_4^- + \tfrac{1}{2}O^{2-} \quad \textbf{(EQ 34)}$$

2. Charge transfer with bonding of the oxide onto carbon surface:

$$O^{2-} + x\,C \rightleftharpoons O{=}C_x \quad \textbf{(EQ 35)}$$

3. Additional entropic energy transfer and/or associated surface structural rearrangement to form carbon monoxide gas:

$$O{=}C_x \Rightarrow CO(g) + (x{-}1)\ C \quad \textbf{(EQ 36)}$$

$$\text{rate} = k_1\ [CO{=}C_x] \quad \textbf{(EQ 37)}$$

The rate constant k_1 for carbon monoxide formation may be controlled by interfacial energy transfer, but this will also depend on the crystalline structure of the carbon with the more disordered carbon structures having a higher rate constant, and lower surface coverage and associated polarization as a given current density.

Electrochemical Formation of Carbon Dioxide

The low Tafel slope resulting when the two processes are enabled supports a second oxide anion being discharged on either the surface intermediate (formed by step 2) or onto the adjacent carbon atom. This would be followed by additional entropic energy transfer and/or an associated surface structural rearrangement:

$$2O{=}C_x \Rightarrow CO_2(g) + (2x{-}1)\ C \quad \textbf{(EQ 38)}$$

$$\text{rate} = k_2\ [CO{=}C_x]^n \quad \textbf{(EQ 39)}$$

The residual entropic energy required for completion of the reaction for forming carbon dioxide is less than half the amount required for forming carbon monoxide at current densities above 0.7 $A{\cdot}cm^{-2}$, while the strained intermediate structure that could result on the carbon crystal lattice would also contribute to the rate constant for carbon dioxide formation being significantly larger.

The combined considerations of the electrode polarization and analysis of anode gases and reaction mechanisms clearly indicate that for normal quality anodes used in the aluminum smelting industry, approximately 5% of the metal is formed by the carbon monoxide mechanism. Therefore, the minimum theoretical carbon consumption is closer to 0.35 kg C per kg Al rather than the 0.333 commonly quoted. Generally, the better baked the carbon anode (higher baking and heat treatment temperature), the less will be the proportion of carbon monoxide formed.

Other Reactions Within the Cell

Table 5 also lists reactions associated with the major impurities in the alumina and carbon raw materials. The dissolved water or hydroxyl arising from the incomplete calcination of the alumina precipitated in the Bayer process is the major source of hydrogen fluoride emitted during continuous operation of the cell. Its electrochemical formation (Equation 4) is enabled at all practical operating current densities, but completion of the reaction requires a greater amount of energy and formation of carbon dioxide. The primary problem of this reaction is the environmental harm that gaseous fluoride emissions cause on plant and animal life. However, the hydrogen fluoride is captured with high efficiency by modern cell designs and nearly qualitatively removed in the dry scrubbing process, so the main impact of this reaction is on the capital cost of the smelter.

The sulfur bound in the anodes is electrochemically oxidized and released as COS(g), but no accurate mass balances have been presented. Other sulfur-containing gases have also been detected while $SO_2(g)$ becomes the dominant sulfurous gas after combustion with air.

Operating Implications of the Cell Reactions

Five major consequences may arise that impact cell operating conditions:

1. The anode potential needs to be constrained below ~1.8 V to prevent the co-evolution of perfluorocarbons.
2. The constraint on the anode potential also introduces constraints on the operating current density and minimum alumina concentration of the cell because of their impact on the electrode polarization and, hence, anode potential.
3. Within the electrode potential constraint operating region, an energy deficit remains for completion of the cell reactions, and consequently, the heat transfer rate from the electrolyte to the anode can be a limiting feature.
4. It is important to minimize spatial variations in cell conditions and properties, as temperature or alumina concentration gradients can change the current density and potential of individual anodes enabling localized perfluorocarbon evolution with minimal change in cell voltage.
5. The quality of raw materials also has an impact on the total energy consumption, because they can enhance the proportion of the electrochemically enabled but thermodynamically unfavorable secondary reactions.

VOLTAGE "AT CELL" AND CELL CONTROL

Operating cells are self-heating, and, therefore, the voltage between the anode beam and cathode current collector bars must be high enough to provide the energy required, when obviously multiplied by cell current, for

1. The energy to preheat all materials—alumina and impurities, gross anode carbon and its impurities, make-up chemicals, and anode cover material—introduced to the cell;
2. The energy required for the state changes of materials that are removed from the cell—such as the hot residual anode butt, and reacted hot anode cover material;
3. The energy for all the conversion reactions; and
4. The heat loss of the cell, which is dependent on cell size but decreases per unit metal production when operating current is increased.

The summation of the first three is the requirements for the conversion process of the raw materials to their final products. As demonstrated in the discussion of the multiplicity of reactions, there are several unavoidable processes compared with the simple value usually assumed for aluminum extraction according to the reaction forming carbon dioxide, which is usually quoted as the base reference situation. As seen in Table 5, these increase the process energy by more than 4%, while the value can also increase with minor variations for different quality raw materials and faradic efficiencies. In the industrial environment, it is more common to discuss energy consumption in terms of kilowatt-hours used per unit production. Through Faraday's law, there is also a correlation between energy and voltage. Consequently, in constructing, three forms of units are presented. Expressing in the terms of voltage is usable for understanding the cell design and operating constraints.

The equivalent voltage needed for the process forms the base requirement, and the other energy input requirement

comes from the cell heat loss. Two important components of the cell voltage that need to be allowed for are the

1. Anode potential—which depends on current density and dissolved alumina concentration, but ideally it should not exceed 1.75 V; and
2. Cathode potential—which is current density and electrolyte composition dependent, but it seldom exceeds 0.1 V.

Beyond these components, the rest of the energy can be provided from heat generated through ohmic resistance of the electrode materials and electrolyte used. As seen in Figure 10, there are three major contributions to the ohmic resistance of a cell, but there are several components contributing to each one. The three contributors are

1. The ohmic voltage drop as a consequence of the resistive components of the anode and its assembly;
2. The ohmic voltage drop as a consequence of the resistance of the cathode lining, its jointing to the steel current collector bar and its resistance; and
3. The ohmic resistance of the electrolyte filling the gap between the two electrode surfaces.

In Figure 10, the electrochemical voltages are shown as voltage-dependent resistance because although current flows across the interface, its magnitude is not proportional to Ohm's law. Also, the electrode has an inductance to maintain the potential gradient, hence the capacitor in parallel.

The final voltage at the cell once the line current is set is determined to give the cell heat balance for the metal productivity to be achieved. Once the various resistive components are set by design (according to constraints discussed below), the adjustable variable that enables the required voltage to be achieved is the resistance of the electrolyte, which is varied by changing the interelectrode separation.

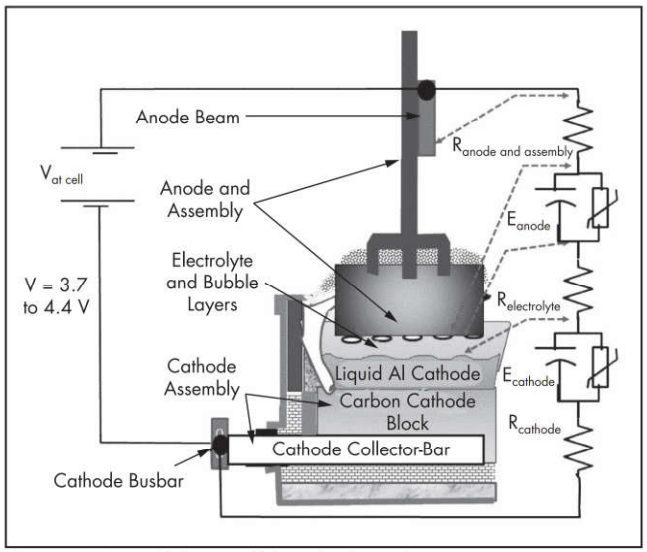

Figure 10 Breakdown of the ohmic resistance components contributing to overall cell voltage

Anode Resistance

Total anode resistance depends on anode size, but also the cross-sectional design of the current-carrying anode assembly, and the interfacial contact resistance generated by the casting between the anode carbon and the terminal anode "stubs" of the current-carrying assembly. The resistance of the anode carbon itself is a variable because of the consumption of the carbon, which brings about a substantial change in the height or depth (typically more than 70% reduction during the life cycle) and lesser changes in the cross-sectional area facing the cathodic surface of the metal pad. Modern anodes tend to have length-by-width geometric areas between 1.0 and 1.4 m^2, and for a 1-m^2 anode base, the total assembled resistance would drop from about 44 to 25 μΩ (micro-ohms) during its life.

Cathode Assembly Resistance

Direct electrical contact with the molten metal cathode is through a series of preformed carbonaceous blocks running across the width of the cell and jointed with the carbonaceous paste that solidifies during the preheating and start-up. All structural metals that withstand the temperature required have too high solubility in aluminum to enable formation of marketable quality aluminum or to give any reasonable service life. Of the electronically conducting refractories, only the diborides of titanium and zirconium have adequate resistance to attack by the metal or electrolyte. But both the costs and the challenges presented by using a refractory material have until now prevented their introduction to operating cells despite many innovative attempts.

Unfortunately, because of the open porosity of the carbon blocks (typically >15%) and penetration in the pores with electrolyte, a series of chemical and electrochemical reactions occur, particularly near the metal interface, causing the carbon block to slowly wear. Consequently, the cross-sectional area of each of these carbon blocks is typically 45–50 cm deep by 45–50 cm wide, but they have low-resistance steel "cathode current collector bars" embedded in them, starting approximately 25 cm below the surface, that are in contact with the liquid aluminum. To minimize the electrical resistance of the total assembly, some of the embedded steel bars also have inserts of copper. The carbonaceous materials used for forming the blocks vary from pitch-bonded calcined anthracite to high-temperature, fully graphitized material, so the resistance of the material varies widely. Very approximately, the cross-sectional area of the preformed carbon blocks matches that of the anode surface, and with design variations the resistance of the completed cathode assembly ranges from 18 to 55 μΩ/m^2.

Electrolyte Resistance

Today, the industry is standardizing on electrolyte compositions of 4.5–6 wt % CaF_2, 9.5 to 12 wt % excess aluminum fluoride, and approximately 2.5 wt % dissolved alumina operating at a temperature between 955° and 965°C. For the average value, the electrical resistivity is approximately 0.45 Ω-cm, but inevitably, the cells have chemistry and temperature swings around this band, and after allowing for that, the range could vary between 0.427 and 0.466 Ω-cm. However, because of the horizontally oriented electrodes, which carry the dominant part of the current, the resistance is split into two parts—a partially bubble-filled layer immediately under the anode surface and a conventional layer for the remainder of the gap between the anode and cathode. Although many texts display the bubble as being dispersed randomly in the electrolyte, the hydrodynamic pressures generated by the higher density of the electrolyte tend to keep the bubbles extremely close to

the electrode surface. Simulation and modeling studies have shown that these bubbles coalesce and release by rolling along but adjacent to the anode surface in surges. Measurements in laboratory cells have demonstrated that, typically, the average surface coverage of the horizontally oriented electrodes when operated at 0.75 $A \cdot cm^{-2}$ is approximately 35%–40%, and the average depth of the bubble layer is approximately 6 mm (Aaberge et al. 1997). However, the coverage reduces substantially with a small inclination of the electrode surface away from horizontal or a reduction in the distance of the travel path. Slotted anodes have been introduced to achieve these benefits and thus reduce the resistance. Ultimately, the anode-to-cathode spacing and cell heat-balance requirements set the working electrolyte resistance.

CONCLUDING REMARKS

The inherent problems of the present technology for aluminum smelting can be directly linked with limitations of materials available for reactor design resulting in a limited cell life (typically less than six years), design constraints associated with both the need to replenish the consumable anodes, and having two liquid layers that are separated by a small difference in density, causing stability problems of the metal layer in the intense magnetic field, plus the slow reaction rate necessitating a large reaction surface area and, consequently, a large number of cells. These lead to the high capital cost and low energy efficiency because of the large heat loss area. These various constraints have also presented barriers to developing alternative processes despite numerous attempts and extensive research and development.

The economic situation for many aluminum producers has been difficult in recent years. But there are positive signs too. The world will continue to need aluminum, and demand will eventually catch up with production. The current weakness and uncertainty in the world economy are weighing on the aluminum price, but there is continued solid future growth in aluminum demand, and about 5% or 6% growth is expected in the next several years. Global demand for primary aluminum is estimated to reach 70 million t/yr by 2020, which would mean *doubling* since 2010.

ACKNOWLEDGMENT

The authors acknowledge the valuable assistance provided by Stephen Lindsay, technical and operating specialist for Alcoa, who reviewed the manuscript draft and assisted with obtaining accurate, up-to-date data.

REFERENCES

Aaberge, R.J., Ranum, V., Williamson, K., and Welch, B.J. 1997. The gas under anodes in aluminium smelting cells part II: Gas volume and bubble layer characteristics. In *Light Metals 1997*. Warrendale, PA: The Minerals, Metals & Materials Society. pp. 341–346.

Bagshaw, A.N., Kuschel, G.I., Taylor, M.P., Tricklebank, S.B., and Welch, B.J. 1985. Effect of operating conditions on the dissolution of primary and secondary (reacted) alumina powders in electrolytes. In *Light Metals 1985.* Warrendale, PA: TMS-AIME. pp. 549–559.

Dewing, E., and van der Kouwe, Th. 1975. Anodic phenomena in cryolite-alumina melts: I. Overpotentials at graphite and baked carbon electrodes, electrochemical science and technology—Technical papers. *J. Electrochem. Soc.* 122(3):358–363.

Dworkin, A.S., Bronstein, H.R., and Bredig, M.A. 1962. Miscibility of metals with salts. VI. Lithium–lithium halide systems. *J. Phys. Chem.* 66:572–573.

Edwards, L. 2015. The history and future challenges of calcined petroleum coke production and use in aluminum smelting. *JOM* 67:308–321.

Haarberg, G.M., Solli, L.N., and Sterten, Å. 1994. Electrochemical studies of the anode reaction on carbon in NaF-AlF_3-Al_2O_3 melts. In *Light Metals 1994.* Warrendale, PA: The Minerals, Metals & Materials Society. pp. 227–231.

Hall, C.M. 1886. U.S. Patent No. 400,766. Serial No. 207,601.

Héroult, P.L.T. 1886. French patent No. 175,711.

Hume, S.M., Utley, M.R., Welch, B.J., and Perruchoud, R.C. 1992. The influence of low current densities on anode performance. In *Light Metals 1992*. Warrendale, PA: The Minerals, Metals & Materials Society. pp. 687–692.

IAI (International Aluminium Institute). 2017. Primary Aluminium Smelting Energy Intensity, Date of Issue: June 30, 2017. World Aluminium website. www.world-aluminium.org/statistics/primary-aluminium-smelting-energy-intensity/#data. Accessed February 2018.

Jain, R.K., Tricklebank, S.B., Welch, B.J., and Williams, D.J. 1983. Interaction of aluminas with aluminium smelting electrolytes. In *Light Metals 1983*. Warrendale, PA: TMS-AIME. pp. 609–621.

Patterson, E. 2002. Hydrogen fluoride emissions from aluminium electrolysis cells. PhD thesis, University of Auckland, New Zealand.

Richards, N.E., and Welch, B.J. 1964. Electrochemistry. In *Proceedings of the 1st Australasian Conference.* Oxford: Pergamon Press.

Tingle, W.H., Petit, J., and Frank, W.B. 1981. Sodium content of aluminium in equilibrium with NaF-AlF_3 melts. *Aluminium* 57:286–288.